Analyzing The Impact Of Energy Efficient ASHRAE Guideline 36 Control Sequences On Demand Flexibility Potential Of Commercial Buildings: A Multi-Region Analysis

Weiping Huang, Armando Casillas, Marco Pritoni, Shreya Agarwal, Rongxin Yin, Anand Prakash, Dre Helmns, Mary Ann Piette

ABSTRACT

Traditional control sequences for HVAC systems in large commercial buildings have historically led to poor energy efficiency. To overcome this issue, ASHRAE has recently published Guideline 36 (G36), a collection of high-performance control sequences aimed at reducing energy consumption and cost for building owners. While these sequences are effective in increasing energy efficiency, their influence on a building's capacity to deliver demand flexibility remains uncertain. Prior research suggests a potential trade-off between energy efficiency and demand flexibility because permanently reducing energy use negatively impacts the available amount of load that can be reduced when responding to grid signals. To investigate this hypothesis, we created Modelica simulation models for an air handling unit with a G36 trim-and-respond sequence, calibrated these models to a fully instrumented experimental building testbed X1A in FLEXLAB, and simulated different demand flexibility scenarios. Counter to expectations, results show that, during a "shed event" with prior pre-cooling, G36 reduces demand by around 3.1 W/m^2 more than the traditional control sequences, at the cost of a reduction in comfort (1.5 °C-hour/day) across five different cities across the United States. Our results provide encouraging evidence that, under the tested conditions, G36 does not decrease demand flexibility. This study should increase the confidence of building owners, designers, and operators who are looking to take advantage of demand flexibility programs while complying with increasingly stringent building energy efficiency standards.

Introduction

Heating, ventilation, and air conditioning (HVAC) systems use a significant amount of energy for large commercial buildings. Energy from space heating and space cooling in commercial buildings in the U.S. accounts for 50% of total energy use (IEA, 2022). Therefore, there is an interest in improving the energy efficiency of HVAC systems. Traditionally, field control sequences of commercial buildings have been inefficient in terms of energy use. Most recently, however, the American Society of Heating, Refrigerating and Air Conditioning Engineers (ASHRAE) published their Guideline 36 (G36) which provides a set of best-in-class guidelines for HVAC systems to achieve a high level of energy efficiency. Simultaneously, with the increasing penetration of intermittent renewable energy like wind and solar that are added to the electric grid each year, there is interest in using HVAC systems to perform demand flexibility (Satchwell et al. 2021). Demand flexibility is the capability of distributed energy resources (DER) to adjust a building's load profile across different timescales in response to utility grid needs (Schiller et al. 2020).

While both improving the energy efficiency for the HVAC systems and letting the HVAC systems perform demand flexibility can help building owners save on energy costs or get compensated through existing demand response programs (FPL 2024; NYSERDA 2024), there is little research on whether increasing the energy efficiency of HVAC systems through G36 will

increase or decrease the HVAC's systems ability to perform demand flexibility. While not directly related to G36, Riker et al. (2014) mentioned that permanently reducing consumption through energy efficiency reduced the available load for demand response. In addition, Gerke et al. (2020) found through simulations that for residential buildings, demand flexibility was significantly decreased when equipment level energy efficiency was increased, or when the envelope insulation of the buildings was improved. Gerke et al. (2020) also used simulations to show that demand flexibility was slightly increased when a particular thermostat setpoint control strategy in residential buildings increased energy efficiency by reducing overall load but increasing peak load, such that there was more peak load to shed through demand flexibility. Liu el al. (2023) discovered through real building data that demand flexibility was decreased when building envelope insulation was improved, but demand flexibility was increased when control strategies were changed, such as lowering the variable air volume (VAV) minimum damper position and enabling air handling unit (AHU) supply air temperature reset.

This paper dives deeper into investigating the following questions: will increasing the energy efficiency of HVAC systems through G36 increase or decrease the HVAC system's ability to perform demand flexibility? How does this change across different climate conditions? This paper hopes to use simulation models calibrated to experimental building performance data to investigate HVAC system behaviors and cost savings information. The intended audience for these results are building HVAC practitioners considering adoption of G36 to serve both energy reduction and demand flexibility goals.

The experimental building performance data that were used for the simulation model calibration are from the X1A building testbed within FLEXLAB, located in Lawrence Berkeley National Laboratory (LBNL) in Berkeley, CA. FLEXLAB is an experimental facility with several building testbeds that can represent different room types, walls, windows, lights, appliances, and occupancy profiles. FLEXLAB is highly instrumented and can record data from many sensors, equipment, and actuators. The unique contributions of this paper include:

- Developed a Modelica simulation model of a full HVAC system, including the AHU, VAVs, and zones, and calibrated this simulation model to previous experimental building performance data in the FLEXLAB X1A experimental testbed.
- Discussed why the G36 energy efficiency control sequences do not conflict with demand flexibility in various U.S. cities with different climate zones.
- Estimated savings of G36 adoption on demand flexibility and energy efficiency for different climate zones, in order to increase the adoption of G36 in the field.

Method

In order to understand the behaviors of an HVAC system with the G36 control sequence, several simulation models were created that mirrored the FLEXLAB X1A experimental testbed. In each of these simulation models, the HVAC design included an AHU serving three VAV boxes, each VAV serving one of the three zones: north zone, core zone, and south zone. The south zone had a large window facing south, while the core zone had no windows, and the north zone had an exterior door. A typical AHU is a type of HVAC system that can be found in large commercial buildings. The zone and equipment configuration is shown in Figure 1 below.

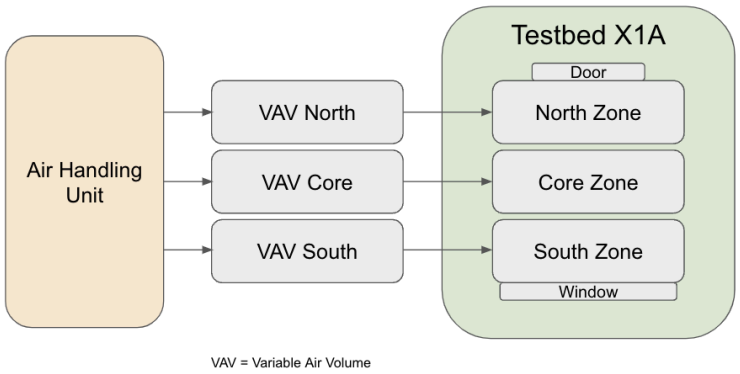

Figure 1: Configuration of experimental testbed X1A in FLEXLAB.

The 2 simulation models represent 2 different control sequences for HVAC systems: a typical non-demand-based control sequence, and a demand-based trim-and-respond sequence from ASHRAE Guideline 36. This study will refer to the typical control sequence as "non-G36" and the Guideline 36 control sequence as "G36" thereafter.

To frame this study, three different demand flexibility strategies were tested. The first one was a baseline, no demand flexibility (no-DF) strategy, where the zone air temperature setpoint was set constant most of the time during the occupied period: 21.1 °C for the heating setpoint and 23.3 °C for the cooling setpoint. 7 am - 10 pm was selected to be the occupied period during a day, and all other hours were defined as the unoccupied period. The second strategy was a load shedding (load-shed) scenario, where during 2pm - 6pm in the occupied period, the zone air temperature cooling setpoint was set higher to 25.6 °C to reduce cooling load. The third strategy was load shifting (load-shift) via precooling, where the zone cooling setpoint was reduced to 22.2 °C between 10 am and 2 pm to cool the zones in advance, followed by increasing the zone cooling setpoint to reduce load during 2pm - 6pm. The zone cooling and heating setpoint during these three demand flexibility strategies across 24 hours are shown in Figure 2. We define the time period between 10 am and 2 pm as the "shift" period, and the time period between 2 pm and 6 pm as the "shed" period. With this definition, the load-shed strategy has a "shed" period, while the load-shift strategy has both a "shed" period and a "shift" period. The zone cooling setpoint was the only difference among these three demand flexibility strategies.

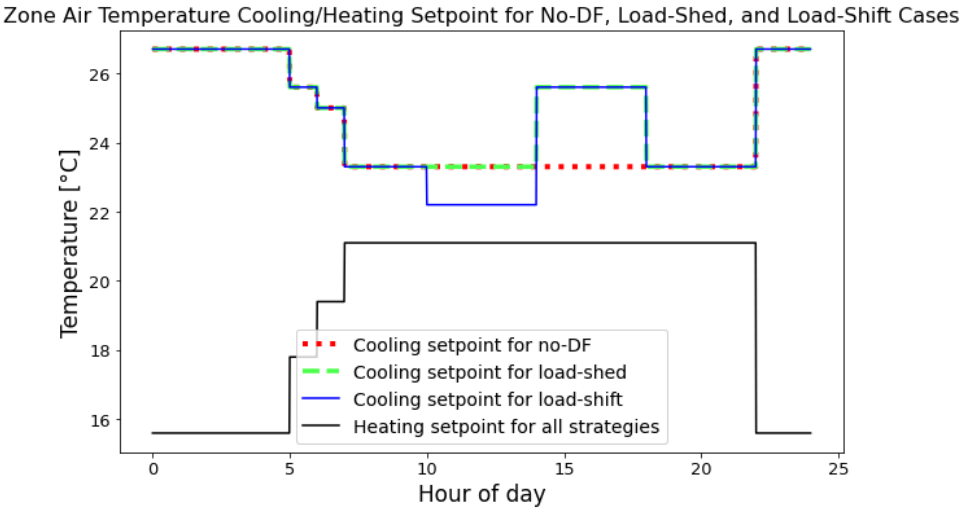

Figure 2: zone cooling and heating setpoints for the no-DF, load-shed, and load-shift strategies.

With three different demand flexibility strategies and two different HVAC control sequences, we formed six test cases: non-G36 + no-DF, non-G36 + load-shed, non-G36 + load-shift, G36 + no-DF, G36 + load-shed, and G36 + load-shift.

Two simulation models were created. Both simulation models used the same HVAC and zone configurations, except that the control parameters were different in order to match the non-G36 and G36 control sequences. For both the non-G36 and the G36 simulation models, users could input different zone setpoints to create the no-DF, load-shed, and load-shift demand flexibility strategies according to Figure 2. The simulation models used the Modelica language in the Dymola software. It used the Modelica Buildings Library (Wetter et al., 2014).

Both simulation models used the same VAV dual max equipment, where the airflow minimum setpoint, the airflow heating maximum setpoint, and the airflow cooling maximum setpoint for the north zone and the core zone were 0.0321 m^3/s, 0.1062 m^3/s, and 0.1062 m^3/s, respectively. The airflow minimum setpoint, the airflow heating maximum setpoint, and the airflow cooling maximum setpoint for the south zone were 0.0496 m^3/s, 0.1062 m^3/s, and 0.1888 m^3/s because the south zone had a south-facing window with direct sunlight exposure, which required a higher cooling load.

Both simulation models used the same internal gain schedule for every day. The internal gain schedule is shown in Figure 3.

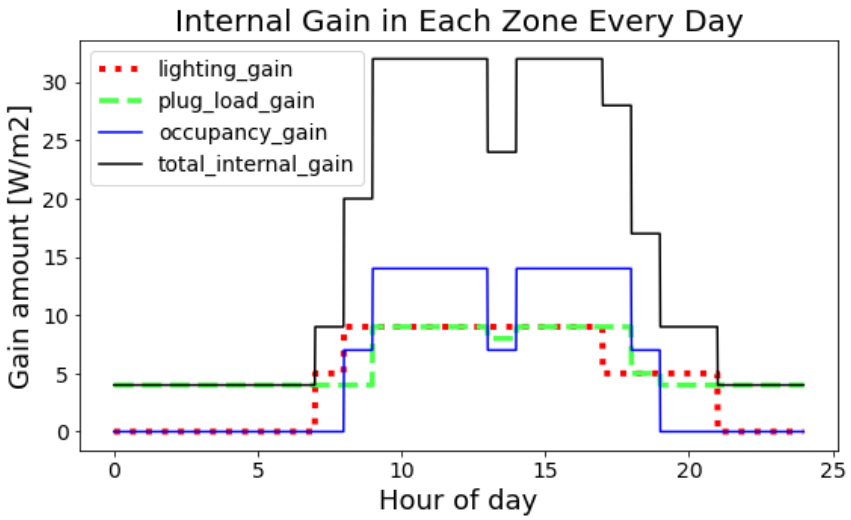

Figure 3: Internal gain schedule for each zone every day.

Trim-and-respond sequence was applied to the supply air temperature setpoint and the supply duct static pressure setpoint during the occupied period for the G36 simulation model only. The supply air temperature setpoint and the supply duct static pressure setpoint for the G36 simulation model during the unoccupied period were set to constant values of 18.3 °C and 25 Pa. The parameters for the trim-and-respond control sequence are shown in Table 1. The trim-and-respond sequence works by generating 0, 1, 2, or 3 requests for each zone served by an AHU system. The number of requests generated in each zone is based on the zone cooling loop signal for the case of supply air temperature setpoint control, or based on the zone VAV damper position for the case of supply duct static pressure setpoint control. For example, if all zones generate a total of 2 requests for the supply duct static pressure setpoint control, since there are 0 ignored requests, the "trim" part of the trim-and-respond sequence would decrease the static pressure setpoint by 12 Pa. While the "respond" part would increase the static pressure setpoint by 50 Pa, twice of the "respond" amount, the maximum response limits the static pressure setpoint increase to 32 Pa. This will cause the static pressure setpoint to increase by a net value of 20 Pa for each time step of 3 minutes.

With the trim-and-respond logic recommended by the G36 specification document (ASHRAE 2018), the trim-and-respond sequence was directly controlling the supply duct static pressure setpoint, while the supply air temperature setpoint control was more involved. When the outdoor air temperature is 21.1 °C and above, the supply air temperature setpoint will be at 11.7 °C. When the outdoor air temperature is 18.3 °C and below, the supply air temperature setpoint will be controlled by the trim-and-respond sequence between 12.8 °C - 18.3 °C. A linear relationship of the supply air temperature setpoint exists when the outdoor air temperature is between 18.3 °C and 21.1 °C. The parameters for the trim-and-respond control sequence are shown in Table 1, and the supply air temperature setpoint trim-and-respond reset logic was illustrated in Figure 4.

Non-G36 + no-DF case did not have the trim-and-respond control sequence; the supply air pressure setpoint maintains at 250 Pa for both the unoccupied period and the occupied period, and the supply air temperature setpoint maintained at 11.7 °C during the occupied period and 18.3 °C during the unoccupied period. The North zone square footage is 19.7 m^2, and core zone and south zone square footage were equivalent at 18.6 m^2. All 3 zones have a height of 2.74 m.

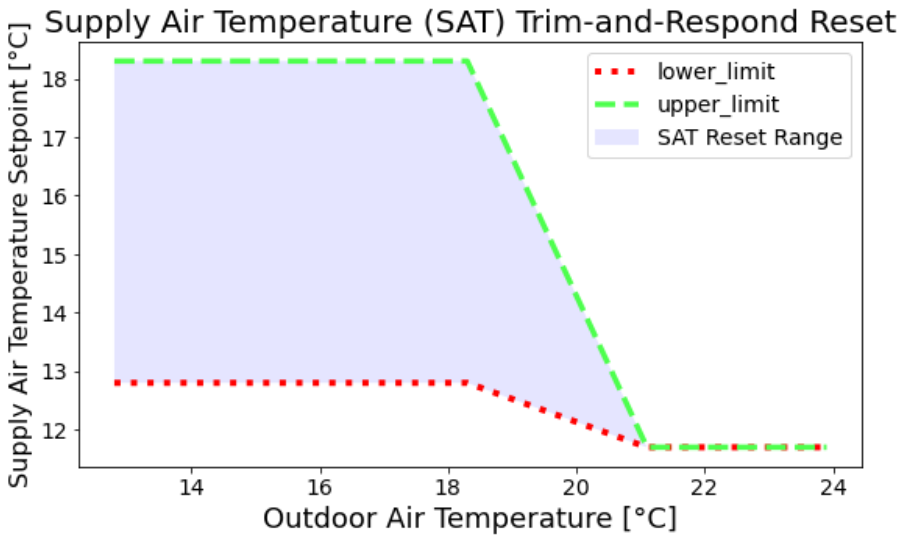

Figure 4: Supply air temperature trim-and-respond reset range and partial dependence on outdoor air temperature.

Table 1: Parameter values used for G36's trim-and-respond control sequences during the occupied period.

Description	Static pressure setpoint	Supply air temperature setpoint (outdoor air temperature < 18.3 °C)
Trim amount	-12 Pa	0.083 °C
Respond amount (must be opposite in sign to the trim amount)	25 Pa	-0.17 °C
Maximum response per time interval (must be same sign as the "respond" amount)	32 Pa	-0.67 °C
Time steps (minutes)	3	3
Number of ignored requests	0	0
Minimum set point	25 Pa	12.8 °C
Maximum set point	250 Pa	18.3 °C

For calibration, existing data from previous experiments in the FLEXLAB X1A testbed was leveraged. In general, a calibration process starts with tuning the parameters in a simulation model and making sure that the setpoints and control sequences of the simulation model align with the actual equipment. Then, the simulation model is run, and simulation results are compared with data from the actual equipment. If the simulation results and the actual equipment data agree with each other based on some calibration metrics, then the calibration process is

complete. If they don't agree, then the simulation parameters need to be re-tuned, and the setpoints and control sequences in the simulation model need to be re-checked in order to re-run the simulation. This forms a full loop of calibration.

The calibration of the simulation models of the FLEXLAB testbed X1A followed the above calibration process. Parameters that were tuned included proportional–integral–derivative (PID) controller time constants, room characteristics such as internal zone air mass capacitance capable of storing sensible heat, and more. Setpoints and control sequences that were checked included AHU supply air temperature and supply duct static pressure trim-and-respond control sequence parameters, VAV discharge air temperature and airflow setpoints, damper and valve commands, and more. The simulation results included data points that represented the state of the system, such as AHU supply air temperature, AHU supply airflow, AHU supply air pressure, zone temperatures, VAV discharge airflows, VAV discharge air temperature, and more.

We selected a subset of data points that were important for this research study; they will be called "key data points" thereafter. Two different metrics were used to compare the same key data points between the simulation results and the FLEXLAB X1A testbed data: coefficient of variation of the root mean square error (CV(RMSE)) and normalized mean bias error (NMBE) aligning with ASHRAE Guideline 14 (ASHRAE 2014). For a successful calibration, when processed both the simulation data and the X1A testbed data to hourly intervals, the CV(RMSE) should stay within 0% and 30%, and NMBE should stay within -10% and 10% according to ASHRAE Guideline 14.

The calibrated model simulated 10 summer days from July 1 to July 10. This time period was chosen to represent typical summer day conditions. For the regional analysis, we selected weather data from 5 different cities, Berkeley, CA; Tampa, FL; Chicago, IL; Victorville, CA; and New York, NY, to represent a wide range of climate conditions as well as seasonal and diurnal variations. The two CA locations were of interest given their location in different investor-owned utility territories (Southern California Edison and Pacific Gas and Electric). Based on the results generated from the Modelica simulation model, several key performance indicators (KPIs) shown in Table 2 were calculated. These KPIs were introduced in Liu et al. (2022).

Table 2: KPIs that were used to analyze the control sequence performance.

KPIs	**Unit**	**Method of calculation**
Daily energy consumption	kWh	Total 24-hr energy consumption. Currently, energy consumption is calculated as the sum of the chiller electric power and the supply fan electric power.
Energy demand during shed period	kW	Average demand on the "shed" period (2 pm-6 pm)
Energy demand during shift period	kW	Average demand on the "shift" period (10 am-2 pm)
Shed intensity	kW	Average demand on the "shed" period (2 pm-6 pm) for the no-DF strategy minus average demand on the same "shift" period (2 pm-6 pm) for the load-shed or load-shift strategy

Shift intensity	kW	Average demand on the "shift" period (10 am-2 pm) for the load-shift strategy minus average demand on the same "shift" period (10 am-2 pm) for the no-DF strategy
Occupant discomfort	°C-hour	$\mu = \sum_{0}^{n} \max(0, ZAT - 24\ °C, 18\ °C - ZAT) * TI$ μ = daily occupant discomfort metric in unit of °C-hour *TI* = time interval of zone air temperature data points in unit of hours (e.g. 0.25 hours or 15 minutes) *ZAT* = zone air temperature n = number of zone air temperature data points between the occupied period of 7 am and 10 pm within a day (a 12-hours period with 0.25 hour data point intervals will have 48 data points)

Results

The calibration results for the non-G36 configuration and the G36 configuration are shown in Figure 5. Most key data points met the Guideline 14 criteria for NMBE and CV(RMSE). The AHU cooling coil load was the most notable key data point that did not meet the CV(RMSE) criteria.

Figure 5: Overview of errors for 14 key data points considered in model calibration for the G36 and the no-G36 control sequences.

Calibrated simulations were performed for the 5 cities between July 1 and July 10, and snapshots of the 10-day averaged simulation data were presented. The 10-day average outdoor air temperature and south zone room air temperature for the G36 + load-shift case for all 5 cities are displayed in Figure 6, along with zone setpoints and the thermal comfort limits for the purpose of calculating occupant thermal discomfort. Figures 7 and Figure 8 show the 10-day average daily energy consumption data, as well as average demand data between the "shift" period of 10 am-2 pm and the "shed" period of 2 pm-6 pm for both the non-G36 and the G36 control sequences. Figure 9 shows the shed intensity and shift intensity across all 6 test cases. Figure 10 shows the occupant discomfort for the south zone across all 6 test cases.

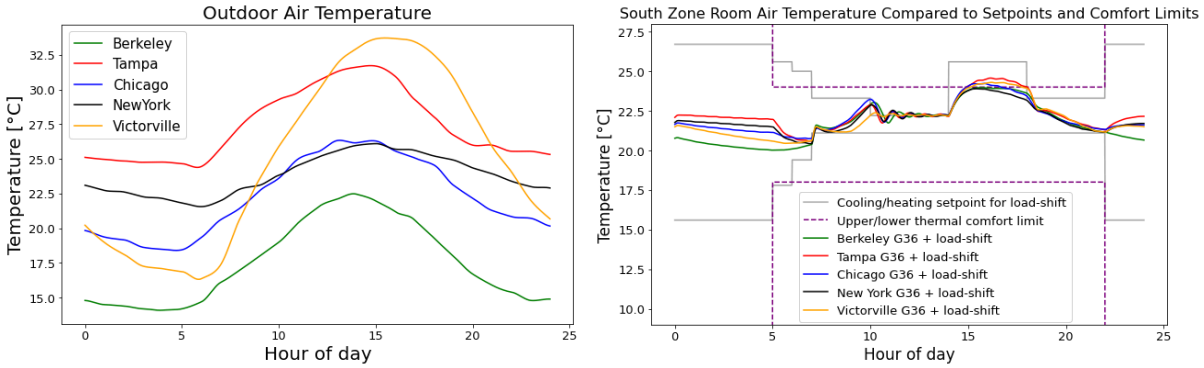

Figure 6: 10-day average outdoor air temperature for all 5 cities, and 10-day average south zone room air temperature compared to setpoints and comfort limits for the G36 + load-shift test case.

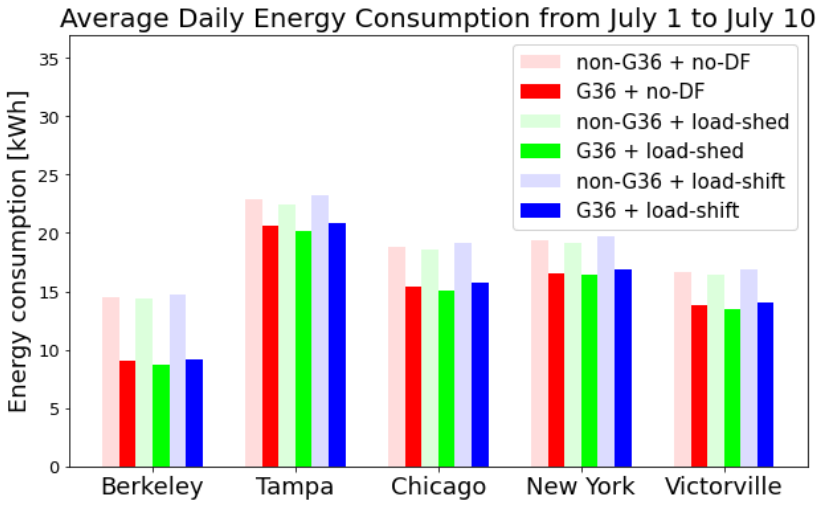

Figure 7: 10-day average daily energy consumption (kWh) for 5 cities.

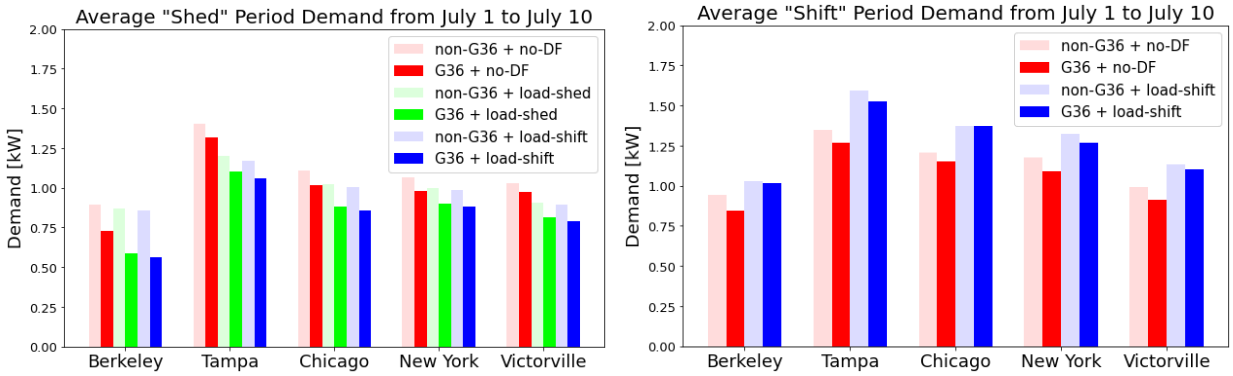

Figure 8: 10-day average "shed" period and "shift" period demand (kW) for 5 cities.

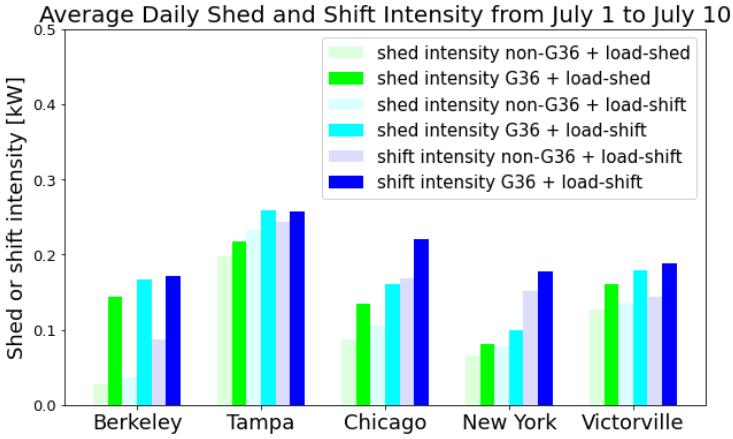

Figure 9: 10-day average shed and shift intensity for 5 cities.

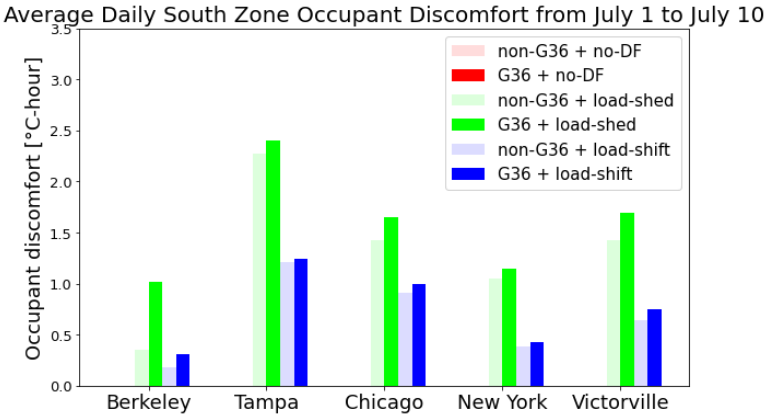

Figure 10: 10-day average south zone occupant discomfort data for 5 cities.

We notice from Figure 7 that Tampa, FL was the most energy intensive, and Berkeley, CA was the least. Thus, we decided to plot data comparisons between these 2 cities. On the other hand, since the load-shift strategy contains both the "shift" period and the "shed" period, the

non-G36 + load-shift and the G36 + load-shift cases were plotted. Figure 11 shows the chiller electric power and the supply fan electric power, which together sum to the total electrical power of the HVAC system. Figure 12 shows the AHU supply air temperature. Figure 13 shows the AHU supply fan airflow rate and the VAV damper position for the south zone. Figure 14 shows the AHU supply fan electric power and the chiller electric power for Berkeley, CA.

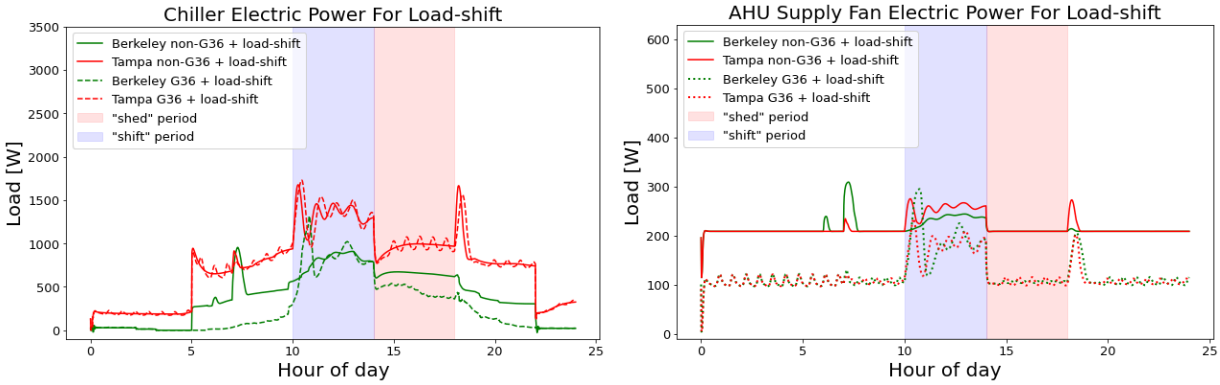

Figure 11: 10-day average chiller electric power and supply fan electric power for Berkeley and Tampa for the load-shift cases.

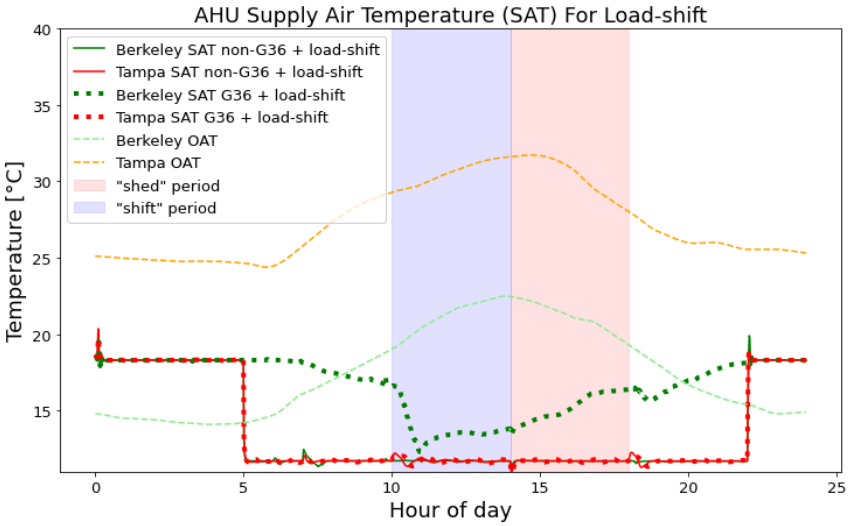

Figure 12: 10-day average supply air temperature for Berkeley and Tampa for the load-shift test cases.

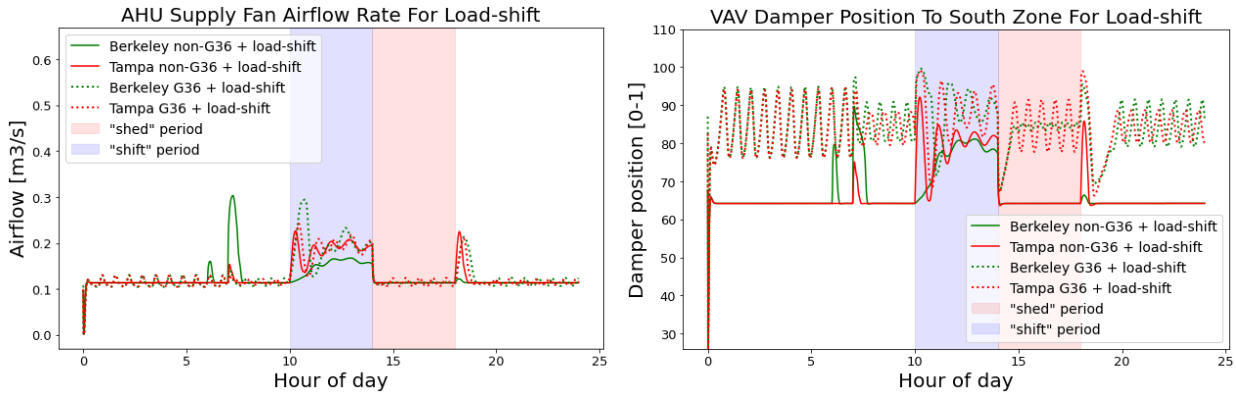

Figure 13: 10-day average AHU supply fan airflow rate and 10-day average VAV damper position for south zone for Berkeley and Tampa for the load-shift strategy.

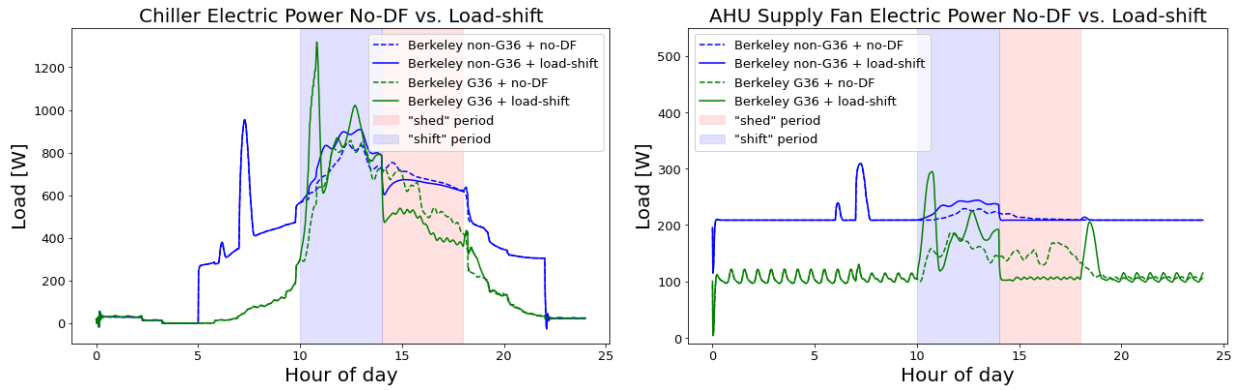

Figure 14: 10-day average chiller electric power and AHU supply fan electric power for Berkeley for the no-DF vs. load-shift cases.

Discussion

The calibration process for the Modelica simulation models of FLEXLAB X1A was largely successful. However, the biggest calibration challenge was calibrating the air temperature of the zones with the building envelope sub-component of the simulation model. This was due to the large number of tunable building envelope parameters, such as internal gains, zone air mass capacitance, wall material characteristics that could not be isolated for further calibration, as well as assumptions related to perfectly mixed zone air in the simulation model. This calibration error caused different discharge airflow conditions in the simulation model, ultimately resulting in different cooling load behaviors. This caused higher error metrics in Figure 5.

Despite different weather conditions for these 5 cities, Figure 7 shows that G36 control sequence was able to reduce daily energy consumption for all 5 cities. We chose to calculate total load to be the sum of the supply fan electric power and the chiller electric power. We see from Figure 11 that G36 was able to reduce the chiller load substantially for Berkeley, but there is barely any load reduction for Tampa. The explanation for these different load reduction behaviors can be found from Figure 12, where the supply air temperature for Tampa was at its minimum value of 11.7°C during the occupied time of 5am - 10 pm, but the supply air temperature for Berkeley was changing between 11.7°C and 18.3°C. This was because the

outdoor air temperature for Berkeley was in the range of the supply air temperature reset range of 18.3°C and 21.1°C, but the outdoor air temperature for Tampa was significantly above 21.1°C. For Berkeley, the supply air temperature trim-and-respond control in G36 set the supply air temperature higher than the supply air temperature for non-G36. The trim-and-respond control would only reduce the supply air temperature when the zones requested it. When zones requested cooling, such as during the "shift" period, the AHU supply air temperature for G36 was slightly higher than non-G36 (Figure 12), meaning that the chiller would only need to achieve a lower temperature delta between the AHU supply air temperature and return air temperature for G36. However, the AHU supply airflow for G36 was also higher than that for non-G36 (Figure 13). A combination of a lower temperature delta and a higher airflow caused the chiller electric power for G36 to be similar to that for non-G36 during the "shift" period (Figure 11). On the other hand, when zones did not request cooling, such as the occupied period excluding the "shift" period, the AHU supply air temperature for G36 was much higher than non-G36 (Figure 12), meaning a much lower temperature delta. However, due to the minimum ventilation requirements, the supply airflow stayed the same at a minimum value for both the G36 and the non-G36 control sequences (Figure 13). A combination of a lower temperature delta and the same airflow caused the chiller electric power for G36 to be much lower to that for non-G36 during times when zones did not request cooling (Figure 11). This shows that the trim-and-respond reset for supply air temperature was working, and G36 helped select a cold enough supply air temperature to achieve energy reduction while not reducing the cooling needs.

Figure 11 shows that the supply fan power was lower for the G36 sequence compared to the non-G36 sequence. This is despite Figure 13 showing that the supply airflow for G36 was slightly higher than non-G36 during the "shift" period, and was the same as non-G36 during the "shed" period. This could be explained by VAV damper position for the south zone in Figure 13. South zone was the most cooling-demanding zone, and the VAV damper position was higher for G36 compared to non-G36. This reduced the pressure drop of airflow, so the supply fan could work less hard, resulting in energy savings. Thus, G36 helps open up the VAV damper positions such that the supply fan reduces unnecessary workload.

From Figure 7 and Figure 9, even though G36 reduced the daily energy consumption for all 5 cities, G36 was able to bring additional shed intensity during the "shed" period.

The conventional understanding is that higher energy efficiency leads to lower demand flexibility because there is less energy demand that can be reduced if the energy demand itself is already low. However, this traditional understanding assumes that energy demand can be decreased in a proportional way to its magnitude, that is, if the demand is higher, there is more potential for shedding. However, Figure 14 shows that this was the case for the non-G36 control sequence during the "shed" period. It clearly shows that even the non-G36 + no-DF case was at a high energy use during the "shed" period, the non-G36 + load-shift case was not able to provide the flexibility to reduce energy demand unlike the G36 cases. This was evident from the previous discussion of Figure 11, Figure 12, and Figure 13 that the non-G36 control sequence didn't have the flexibility to provide the most efficient supply air temperature and static pressure. Therefore, when we say that the energy efficiency of G36 can counterintuitively provide more demand flexibility, what really happens is that the energy inefficient non-G36 control sequence is inherently unable to reduce its cooling load in response to lower downstream zone demand. This is due to constant setpoints within the AHU for the non-G36 control sequence.

From Figure 9, comparing the shed intensity for the load-shed strategy versus the shed intensity for the load-shift strategy, the load-shift strategy allowed a slightly larger energy

reduction during the “shed” period. However, the load-shift strategy required a much larger energy increase during the “shift” period, shown by the shift intensity bars in Figure 9. This shows that the stored thermal energy in the air mass during the “shift” period was quickly lost and was not able to carry significant energy savings during the “shed” period, even with the high wall insulation assumption in the Modelica simulation model. However, Figure 10 shows that the load-shift strategy reduced the exposure of thermal discomfort by half compared to the load-shed strategy for both the G36 and the non-G36 control sequences.

Figure 10 also shows that G36 contributed to more thermal discomfort compared to non-G36, especially for the load-shed strategy. Since our calibrated Modelica simulation model assumed high wall insulation, it was unclear how much a low wall insulation would have increased thermal discomfort for the G36 control sequence. While thermal discomfort is defined as the zone air temperature outside the upper and lower thermal comfort limits during occupied hours (Table 2), Figure 6 shows that the thermal discomfort mainly happened during the 4-hour “shed” period for the load-shift strategy. With the thermal discomfort ranging from around 0.5 °C-hour - 2.5 °C-hour daily, this translates to around 0.12 °C - 0.62 °C of temperature violation during the “shed” period for the load-shift strategy.

Shed intensity for the G36 + load-shift test case ranged from 0.10 - 0.25 kW during the load shed period (Figure 9). While the experimental testbed X1A with all three zones has a square footage of 56.9 m^2, this translates to 1.76 - 4.39 W/m^2 of shed intensity per area for the G36 sequence, with a mean of about 3.1 W/m^2. This is within the range of -2 W/m^2 and 11 W/m^2 for office and retail buildings reported in Liu et al. (2022).

Conclusion and Future Work

To understand whether energy efficiency from the Guideline 36 HVAC control sequence will increase or decrease HVAC system’s ability to perform demand flexibility, we developed Modelica simulation models that were calibrated to previous HVAC experimental data in FLEXLAB testbed X1A for both G36 and non-G36 configurations. We then used the Modelica simulation model to perform simulations on different climate zones and how they impacted how much demand flexibility it could provide during the summer season. We found that the energy efficient G36 HVAC control sequence could actually increase demand flexibility potential compared to the traditional non-G36 control sequence. This counterintuitive result is possible because the non-G36 control sequence is both inflexible and energy inefficient.

When simulation is calibrated to data from a real testbed, it is convenient to assess its performance. One of the next steps is to investigate how relative humidity can affect the HVAC performance through more refined modeling of relative humidity in simulation models. We can simulate demand flexibility in winter days, or more extreme days like the hottest day in a year. We can also simulate how much a low wall insulation building could increase thermal discomfort for the G36 control sequence.

Acknowledgements

This work was supported by the Assistant Secretary for Energy Efficiency and Renewable Energy, Building Technologies Office, of the U.S. Department of Energy under Contract No. DE-AC02-05CH11231. This work was also supported by Southern California Edison under the Award Number CW2242139.

References

ASHRAE (American Society of Heating, Refrigerating and Air-Conditioning Engineers). 2014. *ASHRAE Guideline 14-2014 Measurement of Energy, Demand, and Water Savings*. https://upgreengrade.ir/admin_panel/assets/images/books/ASHRAE%20Guideline%2014-2014.pdf

ASHRAE (American Society of Heating, Refrigerating and Air-Conditioning Engineers). 2018. *ASHRAE Guideline 36-2018 High-Performance Sequences of Operation for HVAC Systems*. https://store.accuristech.com/ashrae/standards/guideline-36-2018-high-performance-sequences-of-operation-for-hvac-systems?product_id=2016214&ashrae_auth_token=4575f9a6-50f4-419e-a6c4-9938cfc20e2d

FPL (Florida Power & Light). 2024. *Demand Response Program*. https://www.fpl.com/business/save/programs/demand-response.html.

Gerke, B. F., C. Zhang, A. Satchwell, S. Murthy, M. A. Piette, E. Present, and R. Adhikari. 2020. "Modeling the Interaction Between Energy Efficiency and Demand Response on Regional Grid Scales Preprint Modeling the Interaction Between Energy Efficiency and Demand Response on Regional Grid Scales." *Preprint*. https://www.nrel.gov/docs/fy20osti/77423.pdf

IEA (International Energy Agency). 2022. *Space Cooling*. Paris: IEA. https://www.iea.org/reports/space-cooling.

Liu, J., L. Yu, R. Yin, M. A. Piette, M. Pritoni, A. Casillas, and P. Schwartz. "Factors Influencing Building Demand Flexibility." 2023. https://doi.org/10.20357/B71882.

Liu, J., R. Yin, L. Yu, M. A. Piette, M. Pritoni, A. Casillas, J. Xie, T. Hong, M. Neukomm, and P. Schwartz. 2022. "Defining and Applying an Electricity Demand Flexibility Benchmarking Metrics Framework for Grid-Interactive Efficient Commercial Buildings." *Advances in Applied Energy* 8: 100107. https://doi.org/10.1016/j.adapen.2022.100107.

NYSERDA (The New York State Energy Research and Development Authority). 2024. *Demand Response Programs*. https://nyserda.ny.gov/All-Programs/Energy-Storage-Program/Energy-Storage-for-Your-Business/Demand-Response-Programs.

Riker, C., K. Wang, and F. Yoo. 2016. "Energy efficiency and automated demand response program integration: Time for a paradigm shift." In *ACEEE Summer Study on Energy Efficiency in Buildings*. https://www.aceee.org/files/proceedings/2014/data/papers/4-912.pdf

Satchwell, A., M. A. Piette, A. Khandekar, J. Granderson, N. M. Frick, R. Hledik, and D. A Nemtzow. 2021. *National Roadmap for Grid-Interactive Efficient Buildings*. Berkeley, CA: Lawrence Berkeley National Laboratory. https://gebroadmap.lbl.gov/

Schiller, S., S. Lisa, and M. Sean. 2020. "Performance Assessments of Demand Flexibility from Grid-Interactive Efficient Buildings: Issues and Considerations." *eScholarship*. https://doi.org/10.2172/1644287.

Wetter, M., W. Zuo, T. S. Nouidui, and X. Pang. 2014. “Modelica buildings library.” *Journal of Building Performance Simulation*, 7 (4): 253-270. https://doi.org/10.1080/19401493.2013.765506